Available online at www.sciencedirect.com
ScienceDirect
Materials Chemistry and Physics 103 (2007) 118–126
MATERIALS CHEMISTRY AND PHYSICS
www.elsevier.com/locate/matchemphys

Poly(vinyl acetate)–clay hybrids prepared via emulsion polymerization, assisted by a nonionic surfactant

M.C. Corobea [a], V. Uricanu [b,*], D. Donescu [a], C. Radovici [a], S. Serban [a], S. Garea [c], H. Iovu [c]

[a] *National R-D Institute of Chemical Research, Splaiul Independentei 202-6, P.O. Box 174/35, 060021 Bucharest, Romania*
[b] *University of Twente, Applied Physics Department/NCV, Postbus 217, 7500 AE Enschede, The Netherlands*
[c] *Polytechnic University of Bucharest, 149 Calea Victoriei, 010072 Bucharest, Romania*

Received 3 March 2006; received in revised form 15 November 2006; accepted 30 January 2007

Abstract

Hybrid materials containing poly(vinyl acetate) and montmorillonite (MMT) were prepared using an *one-batch* emulsion polymerization recipe, assisted by a nonionic surfactant. To explain the results of our experiments, a thorough investigation of the specific interactions between the compounds was done, in the wet as well as the dried state of the end-products. In dispersion, polymer–surfactant interactions were found to be driven by hydrophobic coupling into superficial (mixt) admicelles. Another important finding is that the amount of clay used in the recipes and its relative concentration with respect to the other reaction partners influences drastically the morphological units in the end-products. For low [MMT], well-defined, spherical particles are formed. At the other extreme, for high [MMT], production of polymeric, water-swollen aggregates is favored. A small amount of reformed MMT tactoids was detected in all casted hybrid films, indicating that most of the inorganic is dispersed in the organic phase.

Keywords: Adsorption; Composite materials; Nanostructures; Thermogravimetric analysis

1. Introduction

Recently, polymer–clay hybrid materials have received significant attention because the mutual interactions between polymer and clay are considered to affect their properties. By comparison with conventional microcomposites, greatly improved physical and mechanical characteristics were found for hybrids based on thermoplastic matrices containing a nanoscale dispersion of layered silicates [1–5]. High moduli [6–10], increased strength and heat resistance [11], decreased gas permeability [12–16] and flammability [17–21] and increased biodegradability of biodegradable polymers [22] can be obtained at much lower loads of the inorganic compound, hence decreasing significantly the production costs.

The properties of the hybrid materials are directly related to their internal morphology and, in this respect, the state of dispersion of the inorganic phase is very important [5]. At low clay content, *exfoliated* nanocomposites are encountered. For these composites, individual clay platelets are separated by a continuous, more or less thick polymer matrix. As the inorganic load becomes higher, *flocculated* and/or *intercalated* hybrids are formed.

In practice, the most commonly used 2:1 layered silicates are: montmorillonite, hectorite and saponite. Montmorillonite (MMT) is a hydrated alumina-silicate clay composed of units made up of two silica tetrahedral sheets with a central alumina octahedral sheet. The silicate layers of MMT are planar, stiff, ∼10 Å in thickness, about 2000 Å in length. In nature, MMT clays do not occur as isolated individual units but as crystalline structures (also known as tactoids) formed by aggregation [5,23–26].

The efficiency of the MMT dispersion in a polymer matrix depends strongly on the clay's afinity towards the macromolecular chains and, also, on the MMT tactoid sizes. The hydrophilic nature of the MMT surface impedes their homogeneous dispersion in highly hydrophobic polymer phases. One option to circumvent this drawback is to convert the silicate surface to an organophilic character, by ion-exchange reactions with cationic surfactants. Another possibility is to use directly

* Corresponding author. Tel.: +31 53 489 30 97; fax: +31 53 489 10 96.
E-mail addresses: v.i.uricanu@k.ro (V. Uricanu), ddonescu@chimfiz.icf.ro (D. Donescu).

0254-0584/$ – see front matter © 2007 Elsevier B.V. All rights reserved.
doi:10.1016/j.matchemphys.2007.01.021

the high affinity of the clay for water-soluble polymers, like: poly(ethyleneoxide), poly(vinyl alcohol), poly(vinyl pyridine) or poly(ethylene vinyl alcohol). However, one should always be careful when choosing, since the delicate balance in the clay/polymer's interactions is strongly influenced by the polarity of the solvent(s). The high polarity of water causes swelling of the tactoids and, depending on pH and ionic strength, dispersion into individual units.

In this paper, we explore the possibility to obtain polymer–MMT hybrids using an *one-batch* recipe, with growing of the polymeric phase via a radicalic (emulsion) polymerization, after dispersion of the MMT tactoids in water. The starting monomer is vinyl acetate (VAc) and the reaction is assisted by a nonionic surfactant, with a medium-long (30 units) ethyleneoxide tail. Since both the clay and the growing PVAc particles will compete for the surfactant, we made a thorough investigation of the specific interactions between the compounds. Several experimental techniques were used to elucidate the phenomena taking place in the wet as well as the dried state of the end-products.

2. Experimental

2.1. Materials

Sodium-montmorillonite (Cloisite Na-MMT) was generously donated by Southern Clay Products Inc., USA. Vinyl acetate (VAc, Chimopar, Romania) was purified by rectification. The initiator: ammonium persulphate (LOBA-Feinchemie) and the surfactant: $NPh_{30}EO$ (nonylphenol poly(oxyethylene) with 30 OE units) from ICI, UK, were used without further purification. Poly(vinyl alcohol) (APV, supplied by Nippon Gohsei, Japan), had an average molecular weight of 59,000 and was 88% hydrolysed poly(vinyl acetate).

2.2. Hybrids formulation

In the batch polymerization, the surfactant (10 g $NPh_{30}EO$) was first dissolved in water (200 g). Further on, under continuous stirring, a given amount of the monomer (VAc, 20 g) was added, the mixture was heated up to 65 °C, then the initiator (0.25 g APS) was added. When clay–organic recipes were prepared, the Na-MMT was first mixed with water and equilibrated at room temperature, under stirring, for 1 h, before adding the surfactant. Besides recipes in which all compounds were used, we prepared also clay–surfactant mixtures without addition of the polymerizable partner. The list of all formulations with polymer is given in Table 1.

After preparation, aliquots were taken from all the *wet* phases, deposited on poly(ethylene) sheets and dried room temperature (25 °C), under a mild nitrogen stream, for 2 weeks, followed by 24 h drying under vacuum. Before measurements in the resulting *dried* state, the poly(ethylene) substrate was peeled off. All hybrids with PVAc yielded self-standing films, with no visible cracks or local changes in transparency (hence no macroscopic phase separation).

2.3. Techniques

The hydrodynamic diameters for particles in the final PVAc latex dispersions were determined by dynamic light scattering (DLS), using a NICOMP 370 equipment.

Adsorption isotherms (used to study the interaction between PVAc latex particles and the surfactant in the dispersed phase, when NO clay is present) were determined at 25 °C, by mixing a known amount of the dialysed latex with a constant volume of calibrated surfactant solutions in 50 ml centrifuge tubes. The mixtures were magnetically stirred for 1 h and left to equilibrate. After reaching equilibrium, the mixtures were centrifuged for 45 min at 15,000 rpm. The final concentration of the surfactant in the supernatant was determined spectrophotometrically from the optical density at 276 nm. At this wavelength the absorbance in the UV spectra is due only to the phenyl ring of the hydrophobic head-group.

2.3.1. Dialysis

After synthesis, the PVAc latex was diluted to the desired particle number concentration and dialysed in well-boiled Visking dialysis tubing, against large quantities of distilled water. The water (18 MΩ cm^{-1}, pH 5.7) used for dilution purposes and as dialysis medium was ultrapure deionized water filtered through a Millipore equipment. Dialysis was stopped when the conductivity of the water outside the dialysis tubing was reduced to the value corresponding to the pure water used. The solid content of the colloidal latex (used as stock dispersion) was determined gravimetrically.

Free APV–surfactant aqueous solutions were investigated using viscometry, surface tension (pendant drop method) measurements and DLS.

Termogravimetrical analysis (TGA, with a speed of 20 °C min^{-1}) and differential scanning calorimetry (DSC, 10 °C min^{-1}) were performed with a Dupont 2000 instrument.

X-ray difraction (XRD) studies were done using a DRON-2 instrument with horizontal goniometer and a Cu Kα (λ = 1.5418 Å) radiation source.

After coverage with a thin (20 nm, sputtered) gold layer, the fractured surfaces of the dried polymer–clay composites were observed by scanning electron microscopy (SEM), using a JEOL-5610 equipment operated with a high-tension voltage of 20 kV.

3. Results and discussions

3.1. Interactions between components

For researchers working with MMT's and nonionic surfactants with ethyleneoxide moieties, the subject of specific interactions between the two reagents is probably more familiar. We have chosen to address this subject (in Section 3.1.2) by comparison with the changes induced when PVAc is also present. To understand better what is the role of every compound, we begin by showing what could be expected in a latex–surfactant dispersion, without clay.

3.1.1. Polymer–surfactant

The PVAc particle/water interface is not smooth but hairy, having a layer containing flexible polymer chains terminating in sulphate groups [27–32]. These pendant polymer chains are the key features in determining the adsorption pattern of surfactants and the hydrodynamic diameter of the latex particles [27,33–44]. Adsorption of surfactant molecules onto *hairy polymer latex* particles can be seen as a "localised" polymer–surfactant interaction.

For nonionic surfactants, the published literature reports mainly on the interaction with nonionic polymers [45–49] or hydrophobically modified polymers [50–52]. Thermodynamic calculations [53–55] predict that, if both partners are uncharged, the interaction is either nonexistent, either extremely small. As for ethoxylated nonionic surfactants, they bind easily to polymers that develop hydrogen bondings, such as poly(acrylic acid) and poly(methacrylic acid) [55–62]. In these systems, hydrogen bonding between the carboxylic group of the polymer and the oxygen of the oxyethylene (OE) chain as well as hydrophobic interaction promotes surfactant aggregation on the polymer chain.

The adsorption isotherm of the $NPh_{30}EO$ surfactant onto the PVAc particles shows four distinct regions. For adsorp-

Table 1
Index of the hydrid preparations, with the average diameter for the PVAc particles measured using dynamic light scattering (DLS)

Sample	Na-MMT (g)	Average diameter (nm)	Comments
H0	–	240	Stable latex, no sedimentation/phase separation for more than 3 years
H1	1	337	Stable latex, no sedimentation or phase separation for around 2 years
H2	2.5	383	The latex was stable for ∼8 months after which the lower region starts building a gel-like phase which grows up to 1/3 from the total sample volume
H3	5	753	The dispersion as prepared is extremely viscous and the transition towards a gel starts after 2 weeks. The gelation proceeds for 3 weeks and, at its end, the whole dispersion is gelled

tion at concentrations lower than 7.7×10^{-5} mol l^{-1} (region **a** in Fig. 1), the adsorbed amount (Γ) increases at surfactant addition. A pseudo-plateau (region **b**), for which Γ is more or less constant, follows. Region **c** in the adsorption isotherm begins at concentrations slightly higher than the critical micelle concentration (cmc) of the surfactant in the aqueous phase and corresponds to a dramatically increase of Γ. At [$NPh_{30}EO$] $\geq 4 \times 10^{-3}$ mol l^{-1}, the final plateau in the plot of Γ versus C^{eq} is reached and the adsorption attains saturation.

The complex shape of the adsorption isotherm is very much alike the binding isotherm of an ionic surfactant to a nonionic, *hydrophobically modified* water-soluble polymer (HM-polymer) [63]. For mixtures of HM-polymer and ionic surfactant, the first region in the binding isotherm corresponds to a high affinity *non-co-operative* binding of individual surfactant molecules to the HM-polymer. As the number of surfactant molecules per each adsorption site exceeds one, the binding becomes *anti-co-operative*. Finally, at concentrations above critical aggregation concentration (CAC), there is a self-association of the ionic surfactant to micelles at the polymer. This process is seen as a *co-operative* binding between surfactant and the HM-polymer.

By analogy, the data in Fig. 1 suggest that $NPh_{30}EO$ could be involved in the formation of a *polymer–surfactant* complex at the surface of the PVAc particles.

Different adsorption stages are also reflected in the modifications of the hydrodynamic diameter of the PVAc particles with adsorbed surfactant, as determined by dynamic light scattering (Fig. 2). In the initial stages (regions **a** and **b** in Fig. 1), the adsorption of $NPh_{30}EO$ molecules around the vinyl acetate segments of the PVAc hairs force them to adopt more expanded conformations. The hydrodynamic diameter increases further, up to a maximum value (Fig. 2). When the surfactant concentration is high enough for the *polymer–surfactant* complex formation, the PVAc hairs are included into micellar-like aggregates. At saturation, the hydrodynamic diameter of the PVAc particles with adsorbed surfactant is lower than the initial value, without surfactant.

Preliminary analysis (IR spectroscopy) showed that the dialysed PVAc particles are (as chemical structure) more similar to a copolymer, including both vinylic acetate and alcohol groups. The latest is more hydrophilic than the formers. Such a copolymer structure corresponds to a partially hydrolysed poly(vinyl alcohol) APV polymer.

In order to gain more information on the *surfactant–polymer hairs* complex, surface tension, viscosity and DLS measurements were performed on aqueous solutions with constant amounts of water-soluble APV and variable $NPh_{30}EO$ concentrations. From these experiments, we hoped to learn more about what can indeed happen when $NPh_{30}EO$ interacts with a hairy PVAc particle.

Same general trends were observed, independent on the APV level (0.25 or 1.25 g l^{-1}). In the APV presence, the surface tension values are not equal to those obtained for surfactant solutions without polymer (Fig. 3 and Table 2). The polymer itself influences these values. For (APV + $NPh_{30}EO$) mixtures, T_1 (≡CAC) coincides with association of polymer and surfactant molecules into a complex. At surfactant concentrations equal to T_2', the surfactant binding reaches saturation. In the concentration range between T_2' and T_2, the concentration of *free* (as

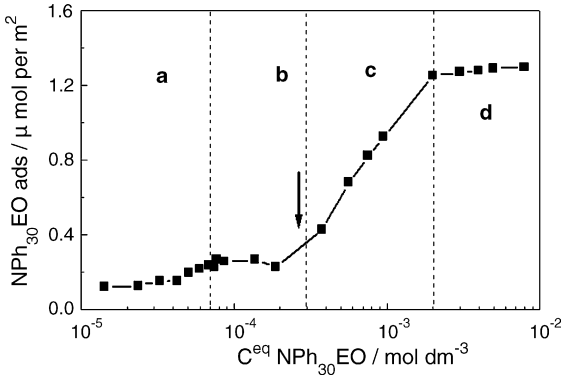

Fig. 1. Adsorption isotherm for nonionic $NPh_{30}EO$ surfactant onto PVAc latex particles. Four distinct regions are clearlly marked; the arrow indicates the *cmc* of the surfactant in the aqueous phase (=2.7×10^{-4} mol dm^{-3}).

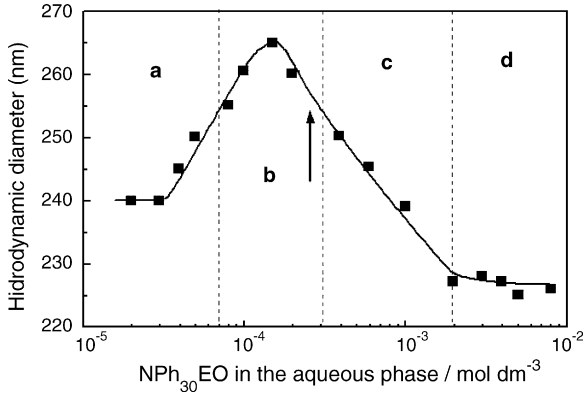

Fig. 2. Hydrodinamic diameter of the PVAc latex particles with adsorbed surfactant.

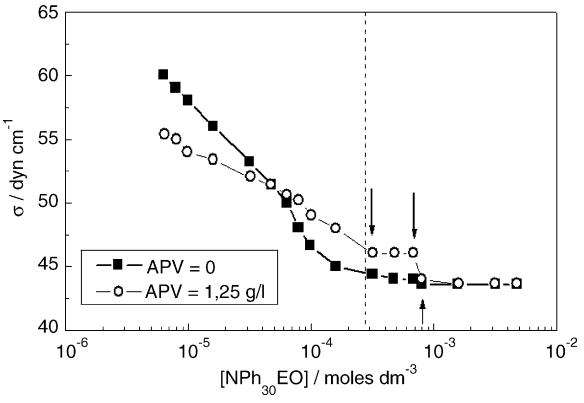

Fig. 3. Surface tension for surfactant solutions with (open symbols) and without APV. The vertical dotted line marks the *cmc* of $NPh_{30}EO$ in pure water. The arrows indicate (from left to right) the T_1 (≡CAC), T_2' and T_2.

Table 2
Values of the surfactant concentrations relevant for changes in the APV–$NPh_{30}EO$ aqueous solutions

[APV] (g l^{-1})	Surfactant concentrations (mol dm^{-3})		
	T_1 (≡CAC)	T_2'	T_2
0.25	4.8×10^{-5}	1.4×10^{-4}	3.0×10^{-4}
1.25	2.6×10^{-4}	6.8×10^{-4}	8.0×10^{-4}

unimers) surfactant molecules increases. Above T_2, the surfactant forms normal micelles in the aqueous phase.

The plot of the reduced viscosity (η_{red}) for solutions with constant APV and variable $NPh_{30}EO$ concentrations (Fig. 4) shows a minimum in the same [$NPh_{30}EO$] range as that for which the surface tension plot (Fig. 3) has its first plateau. This minimum is caused by modifications of the hydrodynamic dimensions of the polymer coil due to formation of APV–surfactant aggregates [64–67]. At [$NPh_{30}EO$] > T_2', the increase in η_{red} results only from the rise in the concentration of pure surfactant micelles, additional to a constant level of APV–surfactant aggregates.

For [APV] = 1.25 g l^{-1} with surfactant, successive measurements of the viscosity revealed a quite interesting behaviour. The values obtained at the first passing of these aqueous solutions through the capillary of the viscometer (η_{red}^{I}) are lower than those obtained at the second measurement (η_{red}^{II}). These discrepancies appear only for $NPh_{30}EO$ concentrations between T_1 and T_2' and higher order measurements recover always the η_{red}^{II} values. Such features of the plot η_{red} versus $NPh_{30}EO$ concentration can be explained by taking into account that, during flow through a capillary, the shear subjects the polymer–surfactant complex to deformations [68].

If the complex does not have a strong binding of the components in the polymer–surfactant mixed aggregates, the local tensions produced by the flow field are responsible for a temporary destruction of the initial geometry of the complex. Time intervals (between two successive viscosity measurements) shorter than the time requested for complex re-equilibration will result in larger η_{red} values. Once the complex achieves more surfactant molecules, its structure becomes more stable against deformation/destruction and the reduced viscosity values are independent on the measurement order.

Dynamic light scattering measurements on (APV + $NPh_{30}EO$) aqueous solutions support the idea of a *polymer–surfactant* complex formation. In the limit of short measurement times, at surfactant concentrations higher than T_1, the hydrodynamic diameter of the *polymer–surfactant* complex (=16.2 nm) is considerable smaller that that of pure APV coil (=32 nm) and very close to the dimensions of the pure $NPh_{30}EO$ micelles (=16.7 nm). In the limit of high measurement times, DLS provides information on the mean diffusion coefficient associated with the slowest movement. For the system investigated, this diffusion coefficient corresponds to an average over all movements at the segmental level of the APV polymer. The formation of mixed *polymer–surfactant* aggregates strongly suppress the segmental motion of the APV chain and the mean diffusion coefficient (Đ) has a sharp decrease at [$NPh_{30}EO$] > T_1 (Fig. 5).

At surfactant concentrations higher than T_2' the experimental values must be subjected to a correction. The physical basis of this correction lies on the changes of the viscosity of the medium

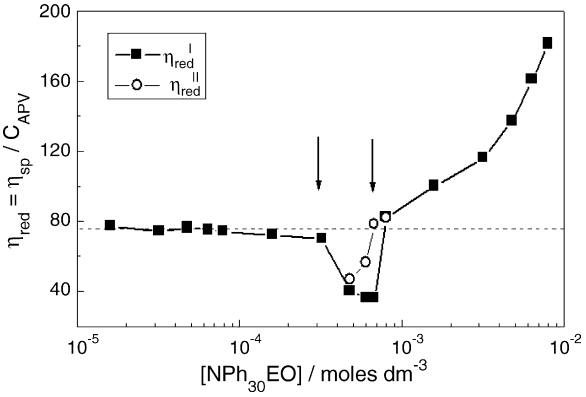

Fig. 4. Variation of APV reduced viscosity in the presence of the nonionic surfactant. The orizontal line represents the η_{red} of aqueous solution with APV = 1.25 g l^{-1} and without surfactant. For surfactant concentrations between T_1 (left arrow) and T_2' (right arrow), the deformation and disruption of the APV–complex give η_{red} values dependent on the measurement order.

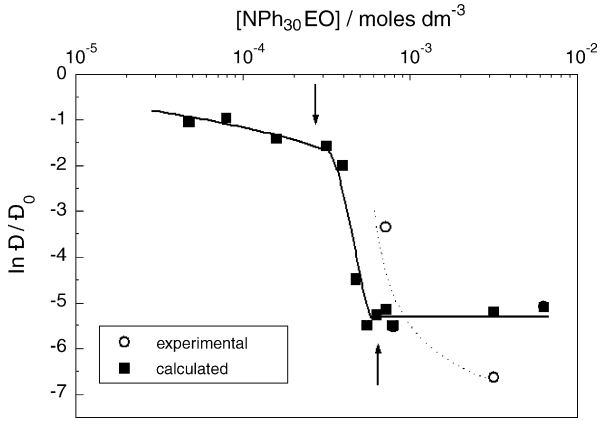

Fig. 5. Variation of the mean difussion coefficient (Đ) for APV with surfactant, as obtained in the limit of long-time DLS measurements. Between T_1 (left arrow) and T_2' (right arrow), the sharp decrease indicates the APV–$NPh_{30}EO$ complex formation.

surrounding the polymer chains. For expanded conformations (in water or with few surfactant molecules, at levels lower than T_1) the APV chain is mainly surrounded by water molecules. In the restricted conformations adopted by the polymer chain in the structure of the APV–$NPh_{30}EO$ complex, in the close proximity of the polymer segments the medium is rich in surfactant molecules. In these conditions, the viscosity term changes its values from that of pure water to that of surfactant aqueous solutions. With these corrections, the plots in Fig. 5 suggest that, in static conditions, the APV–surfactant aggregates have stable structures.

From all the data presented in this section, we can conclude that the $NPh_{30}EO$ molecules have a high affinity to interact with the PVAc latex via hydrophobe–hydrophobe interactions. Here we would like to add few comments. All the experiments done with PVAc latex and surfactant have used an already prepared latex. This means that the interactions evidenced by our investigations would play a crucial role *after* (*or in the latest stages*) of the emulsion polymerization. In the initial stages, since we start to add the polymerizable monomer to an already dispersed clay and $NPh_{30}EO$, the interactions between these last two components will impose perhaps a different path on the polymer formation and (particles) growth.

In the final product, the average hydrodynamic diameter of the PVAc latex particles (see Table 1) was affected by the amount of MMT used in formulation. The ascendent trend could have two explanations:

(i) for higher [MMT], more $NPh_{30}EO$ is involved in the interaction with the clay, leaving less surfactant available for particle stabilization. In this case, the reaction will favor the formation of a smaller number of particle, but with bigger diameters, or
(ii) physical (clay–surfactant–polymer) interactions tend to destabilize the dispersion and, instead of independent latex particles, the DLS measures aggregates.

3.1.2. *Clay–surfactant and clay–PVAc interactions*

For the clay–surfactant interaction, the hydrophilic tail of the surfactant is important [5,69,70]. The chemical structure (ethoxyl groups) of the tail favors ion-dipole and hydrogen bonding of the oxygen atoms with the 2:1 clay. These specific interactions have been already exploited in making hybrids with: EO-surfactants [69,70], EO-monomers [71] or with PEO as pure polymer [7,72–75] or as copolymer [76–78].

Our results (see Fig. 6) confirm the high-adsorption of $NPh_{30}EO$ onto the clay, in agreement with previously published data [79]. When the surfactant–MMT mixtures are dried, one can also estimate (from the position of the (0 0 1) peak in the XRD pattern) the modifications in the basal spacing of the montmorillonite due to $NPh_{30}EO$ insertion between the platelets.

Compared with the initial 12.5 Å value, a swollen state, with higher interlamellae distances = 18 Å is found for all compositions (Fig. 7). This value increases even more (i.e., 20 Å) if the PVAc chains are in the dried mixture. Also, the intensity of the XRD main diffraction peak decreases very much, which suggests a rather small percentage of the reformed tactoids in the films. The small increase in the interbasal spacing in the composite films excludes the existence of 'sandwiches' in which both polymer and surfactant are trapped simultaneously in the clay inner-galleries. Actually, it seems that in the hybrids there is a preferential interaction of the macromolecular chains with the clay surface and we detect exactly its influence via the XRD diffraction paterns.

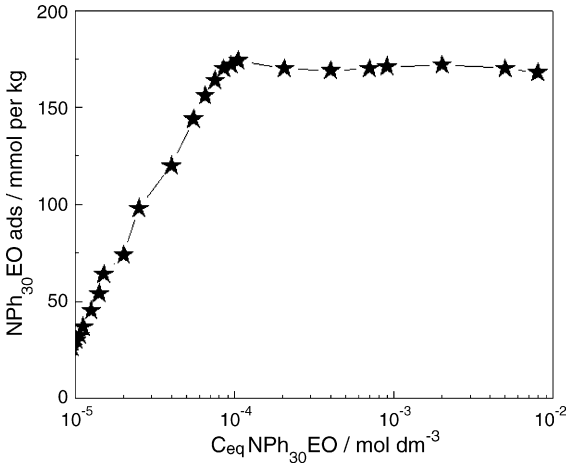

Fig. 6. Adsorption isotherm (Langmuir-type) for the surfactant onto Na-MMT.

Also, the endothermic peaks of the surfactant become less prominent and almost disappeared (see Fig. 8a) in the DSC curves obtained on the dried hybrids. The same was observed also for clay–surfactant mixtures (data not shown). These trends could be explained by a decrease of the ordered association of the $NPh_{30}EO$ molecules in the presence of the other components, saying that the surfactant chains are highly constrained by the presence of Na-MMT and/or PVAc. If one assumes that the melting enthalpy per unit mass of the *free*-surfactant has the same value in all the physical mixtures and polymer-containing composites, the DSC method provides an alternative to calculate the amount of *free*-surfactant, in the dried state. The results are ploted in Fig. 8b. As the inorganic/surfactant ratio increases, a saturation is reached in the amount of *free*-surfactant. When the

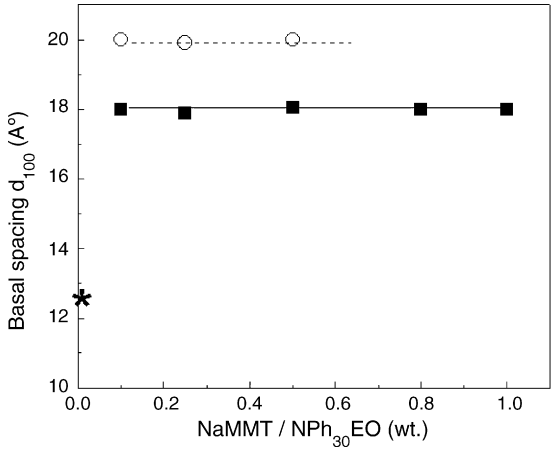

Fig. 7. Basal spacing ($d_{0\,0\,1}$) for dried $NPh_{30}EO$–Na-MMT mixtures (full smbols) and for hybrids with surfactant and PVAc (open symbols). The value measured for pure Na-MMT is indicated by the star.

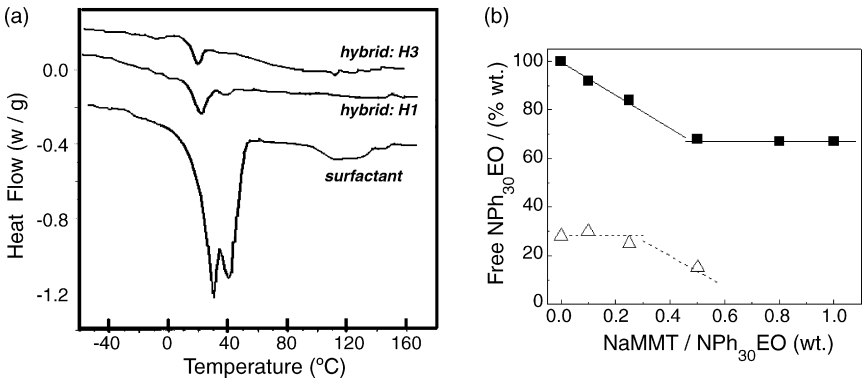

Fig. 8. Results of the films analysis using differential scanning calorimetry (DSC). (a) DSC curves measured for the pure surfactant and the hybrids H1 and H3. (b) Calculated free-surfactant which remains unconstrained by the interaction with the other compounds, for physical mixtures (close symbols) or hybrids (open symbols).

mixtures have also polymer, the saturation was not seen for the compositions used in the present work.

Exploring further the composite films, we used FTIR spectroscopy to get more evidence for mutual inter-elements interactions. The typical bands for the Na-MMT groups [80] were found in the FTIR spectra of pure inorganic phase (Fig. 9): the Si–O (1070 cm^{-1}) and Al–O (524 cm^{-1}) stretching and Si–O bending (at 466 cm^{-1}).

For poly(vinyl acetate) in the H0 formulation, one can easily recognize the peaks of the polymer: a very strong peak at 1736 cm^{-1} (C=O) and the signature for the CH_3C=O, at 1374 and 606 cm^{-1}, associated with a weak doublet: 629–650 cm^{-1} [81]. Adding clay in the preparation recipe changes the interaction balance and, in films, we have direct evidence for a hindering in the vibrations (see also Table 3). More clay in the hybrid induces a strong reduction of the vibrations for the CH_3C=O and the blocking of the O–CH_2 group (vibration located at 1415 cm^{-1}).

It was proven that the interaction of MMT with fully hydrolised poly(vinyl alcohol) is driven by hydrogen bonding between the vinyl alcohol group of the PVA and the silicate oxygens, hence dominating the cleavage plane of the clay [82–85].

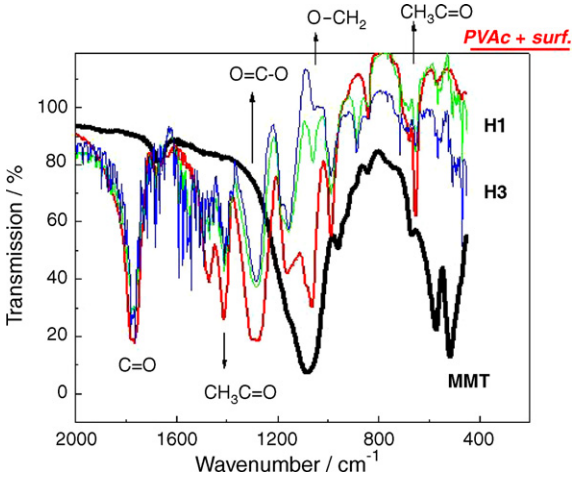

Fig. 9. Selected FTIR spectra for the inorganic (thick line) and the hybrids: H0 (=PVAc + surfactant), H1 and H3.

Our FTIR results (Fig. 9 and Table 3) indicate that also the ester group of the vinyl acetate interacts strongly with the surface of MMT platelets.

The thermal stability of the surfactant (pure or with clay) and of the composite films was determined by TGA as weight loss during a programmed heating. As observed in Fig. 10a, the pure $NPh_{30}EO$ exhibits two weighted-loss steps. The first step, around 270 °C (peak I in Fig. 10a), can be attributed to degradation of chains in amorphous conformations. The second degradation (peak II), with the maximum at ~360 °C, corresponds to surfactant in cristalline arrangements. When in mixture with Na-MMT, a third degradation step occurs (peak III in Fig. 10b), confirming the existence of surfactant entrapped between the clay lamellae.

For a PVAc latex prepared with surfactant and without inorganic, the degradation of the polymeric chains (peak IV, ~410 °C; Fig. 10c) can be easily distinguished from the surfactant contribution. However, in hybrids, we are faced with an interesting situation. The PVAc-contribution is shifted to lower temperatures and we find a combined peak (peaks II + IV; Fig. 10d). The effect (of a less thermally stable polymer) was seen before [86] and can be attributed to a less polymerized structure of the PVAc in the final composite. It means that in hybrids with high clay concentration (as H3), the molecular weight of the polymeric chains is lower than in formulations with none or low clay amounts. In all DTA curves, the thermal degradation ends with a more or less detectable contribution (peak V)

Table 3
Effects of the mutual interactions inside the composite films, as seen in the FTIR spectra

Sample	Location of FTIR peaks (cm^{-1})				Peaks intensity ratios	
	1736	606	524	466	I_{1736}/I_{606}	I_{1736}/I_{524}
Na-MMT	–	W	S	S	–	–
$NPh_{30}EO$	–	v.W	–	–	–	–
Pure PVAc	S	S	v.W	–	1.25	–
H1	S	W	W	W	1.7	3
H2	S	W	W	W	3	3.6
H3	S	W	W	W	4.5	5

The symbols indicate: S, strong; M, medium; W, weak bands.

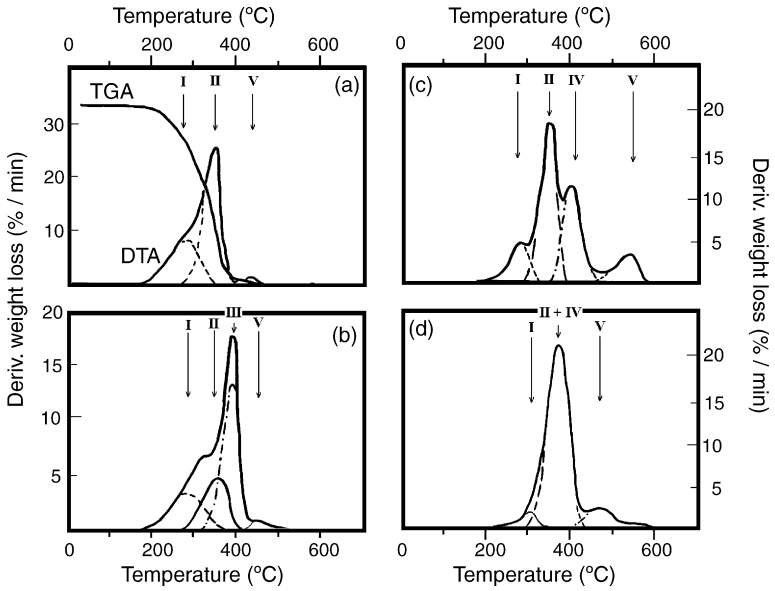

Fig. 10. Derivative thermogravimetric analysis (DTA) on the dried samples for: (a) pure surfactant, (b) surfactant with clay, (c) PVAc latex polymerized with surfactant and (d) hydrid H3, containing polymer, surfactant and clay. For the mixtures in (b and d), the same ratio: Na-MMT/$NPh_{30}EO$ = 0.5 was used. To simplify the graphs, we have included the original TGA curve only in (a). The arrows indicate the positions of the major degradation peaks, as found after deconvolution.

from structure (i.e., ashes) collapse, with burning of the former 'protected' organics [86].

Inspecting (with scanning electron microscopy) the fractures of the composite films (see Fig. 11), we encountered a variable morphology, clearly depending on the amount of Na-MMT used in the initial formulations. Since all the films have an identical fabrication history, the differences in the SEM images could only be explained by a variation in the 'starting units', as explained in what follows.

The PVAc has a low T_g (≈27.5 °C) and, as seen, particles obtained via emulsion polymerization of the vinyl acetate monomer are hairy. Also, when casting the films, the surfactant has a plastifying effect. When films are cast at room temperature, the above-mentioned factors contribute synergetically to partial fusion of the latex spheres. Remains of the initial particles can be still recognize in the fracture of the H0 film (Fig. 11a). As the clay amount increases, there is a visible transition to smoother fractures (Fig. 11c).

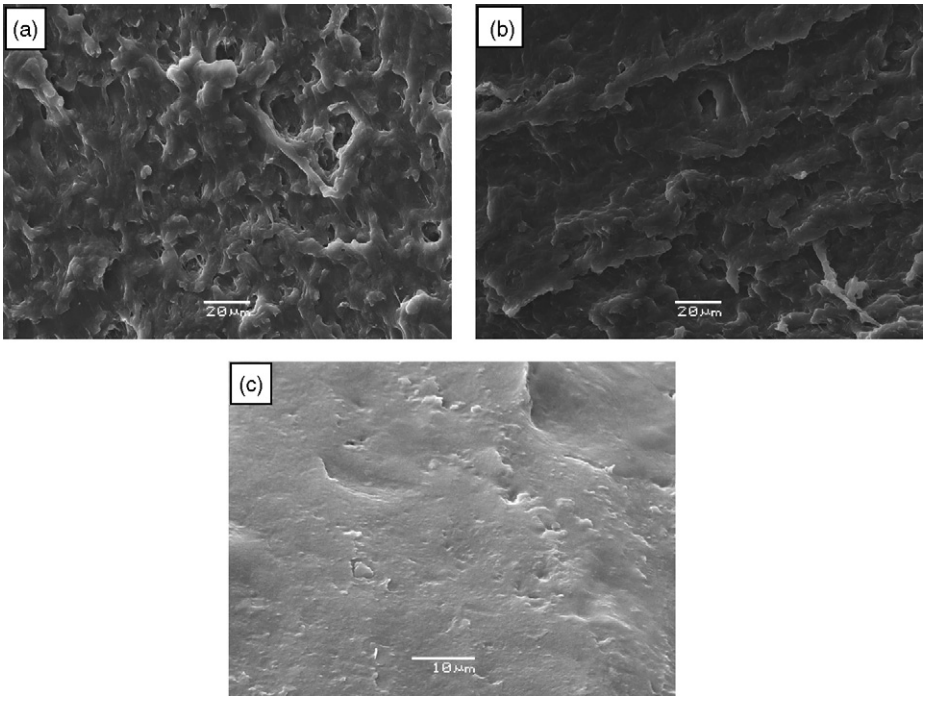

Fig. 11. Scanning electron microscopy images for the composites: H1 (a), H2 (b) and H3 (c), in fractures.

Based on all the data obtained using different analysis techniques in the wet phase (DLS, adsorption isotherms) and dried films (SEM, TGA, FTIR, DSC and XRD), one can advance a coherent scenario which explains all the experimental findings.

In normal emulsion polymerization of vinyl acetate with nonionic surfactant, at the end of the reaction, a good dispersion of spherical (hairy) particles is obtained. These particles show a rather narrow size distribution and have an average hydrodynamic diameter ≈240 nm. Casting films from PVAc latexes will result in films with only partial preservation of spherical units.

If increased amounts of Na-MMT are added in the formulations, a collection of physical interactions drive the system. Multiple effects could be then expected. The clay–$NPh_{30}EO$ interaction, with a direct contact between the ethylene oxide and the inorganic surfaces, gives an increased hydropbobe character to the MMT platelets. We cannot exclude that an increased hydrophobicity would actually make the platelets more attractive as interaction partners for vinyl acetate groups, as monomer or as growing polymeric chains.

Also, due to clay–surfactant initial coupling, there is less surfactant left in the aqueous phase (hence the DSC results; Fig. 8a and b). This turns the balance during the polymerization towards formation of larger latex particles (like in H1, H2; see Table 1) or even PVAc spheres with a high water/polymer ratio. These last entities are more close to super-swollen polymer aggregates than to classical, dense polymeric spheres. Such entities will have larger diameters (see the DLS result for formulation H3) and will shrink and fuse very easily when dried (see SEM image in Fig. 11c). Also, these large units use some of the PVAc chains for stabilization, which increases the probability of interaction with surfactant (i), with clay–surfactant complexes (ii) and eventual bridging via *free PVAc chains* (iii). Since the monomer has a relative high solubility in water: ∼2%, polymerization in the aqueous phase will always provide a certain percentage of free PVAc molecules. Further, if they grow beyond a critical length, these oligomeric molecules will collapse in aggregates, or interact with other partners (like single or surfactant-modified clay platelets). The diversity (in structure) at the end of the polymerization step in formulations with high clay content (as in H3) is the base for a completely different reological properties. In this case we do not have a latex comprized from individual, well-dispersed units, but rather a mixture of elements with a high tendency for associative interactions. The H3 formulation is the extreme example (from the recipes used in the present work) for a mixture which is very viscous and turns relatively soon (2–3 weeks) after preparation into a whole gel (see Table 1).

4. Conclusions

From the results so far obtained, it can be concluded that polymer–clay nanocomposites can be successfully synthesized using a smectic clay, modified by interaction with nonionic surfactant, by a simple emulsion polymerization technique. The amount of clay used in the recipes: (i) and its relative concentration with respect to the other reaction partners (ii) incline the reaction equilibria in different directions. Hence, in the final dispersions, the morphological units could belong to a variaty of forms, spread between: well-defined, spherical particles at one extreme and polymeric, water-swollen aggregates at the other extreme. Most probably, at intermediate MMT concentrations, combinations between the two extremes will be found. A small amount of reformed tactoids was detected in all casted hybrid films, indicating that a large percentage of the inorganic is dispersed in the organic phase.

References

[1] J. Solc, K. Nichols, M. Galobaedes, E.P. Giannelis, Proceedings of SPE ANTEC'97, 1997, p. 1931.
[2] A. Akelah in, P.N. Prasad, J.E. Mark, T.J. Fai (Eds.), Polymer and Other Advanced Materials: Emerging Technologies and Business Opportunities, Plenum Press, New York, 1995.
[3] A. Akelah, A. Moet, J. Appl. Polym. Sci.: Appl. Polym. Symp. 55 (1994) 153.
[4] E.P. Giannelis, Adv. Mater. 8 (1) (1996) 29.
[5] S. Sinha Ray, M. Okamoto, Prog. Polym. Sci. 28 (2003) 1539.
[6] A. Okada, M. Kawasumi, A. Usuki, Y. Kojima, T. Kurauchi, O. Kamigaito, in: D.W. Schaefer, J.E. Mark (Eds.), Polymer Based Molecular Composites, MRS Symposium Proceedings, vol. 171, Pittsburgh, 1990, p. 45.
[7] E.P. Giannelis, R. Krishnamoorti, E. Manias, Adv. Polym. Sci. 138 (1999) 107.
[8] P.C. LeBaron, Z. Wang, T.J. Pinnavaia, Appl. Clay Sci. 15 (1999) 11.
[9] R.A. Vaia, G. Price, P.N. Ruth, H.T. Nguyen, J. Lichtenhan, Appl. Clay Sci. 15 (1999) 67.
[10] M. Biswas, S. Sinha Ray, Adv. Polym. Sci. 155 (2001) 167.
[11] E.P. Giannelis, Appl. Organomet. Chem. 12 (1998) 675.
[12] R. Xu, E. Manias, A.J. Snyder, J. Runt, Macromolecules 34 (2001) 337.
[13] R.K. Bharadwaj, Macromolecules 34 (2001) 1989.
[14] P.B. Messersmith, E.P. Giannelis, J. Polym. Sci. Part A: Polym. Chem. 33 (1995) 1047.
[15] K. Yano, A. Usuki, A. Okada, T. Kurauchi, O. Kamigaito, J. Polym. Sci. Part A: Polym. Chem. 31 (1993) 2493.
[16] Y. Kojima, A. Usuki, M. Kawasumi, Y. Fukushima, A. Okada, T. Kurauchi, O. Kamigaito, J. Mater. Res. 8 (1993) 1179.
[17] J.W. Gilman, T. Kashiwagi, J.D. Lichtenhan, SAMPE J. 33 (1997) 40.
[18] J.W. Gilman, Appl. Clay Sci. 15 (1999) 31.
[19] F. Dabrowski, M. LeBras, S. Bourbigot, J.W. Gilman, T. Kashiwagi, Proceedings of the Euro-fillers'99, Lyon-Villeurbanne, France, September 6–9, 1999.
[20] S. Bourbigot, M. LeBras, F. Dabrowski, J.W. Gilman, T. Kashiwagi, Fire Mater. 24 (2000) 201.
[21] J.W. Gilman, C.L. Jackson, A.B. Morgan, R. Harris, E. Manias, E.P. Giannelis, M. Wuthenow, D. Hilton, S.H. Phillips, Chem. Mater. 12 (2000) 1866.
[22] S. Sinha Ray, K. Yamada, M. Okamoto, K. Ueda, Nano Lett. 2 (2002) 1093.
[23] A. Blumstein, J. Polym. Sci.: Part A 3 (1965) 2653.
[24] S.D. Burnside, E.P. Giannelis, Chem. Mater. 7 (1995) 1597.
[25] M. Sikka, L.N. Cerini, S. Ghosh, K.I. Winey, J. Polym. Sci.: Part B: Polym. Phys. 34 (1996) 1443.
[26] Y. Kojima, A. Usuki, M. Kawasumi, A. Okada, T. Kurauchi, O. Kamigaito, J. Polym. Sci.: Part A: Polym. Chem. 31 (1993) 1755.
[27] V. Uricanu, J.R. Eastman, B. Vincent, J. Colloid Interface Sci. 233 (2001) 1.
[28] A.G. van der Put, B.H. Bijsterbosch, J. Colloid Interface Sci. 92 (1983) 499.
[29] Th.J.J. van der Hoven, B.H. Bijsterbosch, Colloid Surf. 22 (1987) 187.
[30] B.R. Midmore, R.J. Hunter, J. Colloid Interface Sci. 122 (1988) 521.
[31] R.S. Chow, K. Takamura, J. Colloid Interface Sci. 125 (1988) 226.
[32] M. Elimelech, C.R. O'Melia, Colloid Surf. 44 (1990) 165.
[33] W. Brown, J. Zhao, Macromolecules 26 (1993) 2711.
[34] J. Zhao, W. Brown, Langmuir 10 (1994) 3395.
[35] J. Zhao, W. Brown, J. Colloid Interface Sci. 169 (1995) 39.
[36] W. Brown, J. Zhao, Macromolecules 28 (1995) 2103.

[37] J. Zhao, W. Brown, J. Colloid Interface Sci. 170 (1995) 607.
[38] W. Brown, J. Zhao, Langmuir 11 (1995) 1840.
[39] J. Zhao, W. Brown, J. Phys. Chem. 99 (1995) 15215.
[40] J. Zhao, W. Brown, J. Phys. Chem. 100 (1996) 3775.
[41] J. Zhao, W. Brown, Langmuir 12 (1996) 1141.
[42] J. Zhao, W. Brown, J. Phys. Chem. 100 (1996) 5908.
[43] J. Zhao, W. Brown, J. Colloid Interface Sci. 179 (1996) 255.
[44] J. Zhao, W. Brown, J. Colloid Interface Sci. 179 (1995) 281.
[45] X.B. Li, Z.C. Lin, J. Cai, L.E. Scriven, H.T. Davis, J. Phys. Chem. 99 (1995) 10865.
[46] S. Panmai, R.K. Prud'homme, D.G. Peiffer, Colloid Surf. A 147 (1999) 3.
[47] A.K. Panda, A. Chakraborty, J. Colloid Interface Sci. 203 (1998) 260.
[48] J.C. Brackman, N.M. van Os, J.B.F.N. Engberts, Langmuir 4 (1988) 1266.
[49] F.M. Winnik, Langmuir 6 (1990) 522.
[50] K. Thuresson, B. Lindman, B. Nystrom, J. Phys. Chem. 101 (1997) 6450.
[51] J. Appell, G. Porte, R. Rawiso, Langmuir 14 (1998) 4409.
[52] G. Bokias, Polymer 42 (2001) 3657.
[53] E. Ruckenstein, G. Huber, H. Hoffman, Langmuir 3 (1987) 382.
[54] R. Nagarajan, Colloid Surf. 13 (1985) 1.
[55] R. Nagarajan, J. Chem. Phys. 3 (1989) 1980.
[56] S. Saito, in: M.J. Schick (Ed.), Nonionic Surfactants. Physical Chemistry, Marcel Dekker, New York, 1987, p. 881.
[57] S. Saito, J. Colloid Interface Sci. 158 (1993) 77.
[58] V.Y. Baranovsky, S. Shenkov, G. Borisov, Eur. Polym. J. 29 (1993) 1137.
[59] S. Saito, J. Colloid Interface Sci. 165 (1994) 505.
[60] D.F. Anghel, S. Saito, A. Baran, A. Iovescu, Langmuir 14 (1998) 5342.
[61] D.F. Anghel, F.M. Winnik, N. Galateanu, Colloid Surf. A 149 (1999) 339.
[62] I.D. Robb, P. Stevenson, Langmuir 16 (2000) 7168.
[63] B. Jonsson, B. Lindman, K. Holmberg, B. Kronberg, Surfactants and Polymers in Aqueous Solution, John Wiley & Sons, Chicester, 1998.
[64] Y. Mylonas, K. Karayanni, G. Staikos, M. Koussathana, P. Lianos, Langmuir 14 (1998) 6320.
[65] G. Staikos, Macromol. Rapid Commun. 16 (1995) 913.
[66] J. Francois, J. Dayantins, J. Sabbadin, Eur. Polym. J. 21 (1985) 165.
[67] S. Saito, K. Kitamura, J. Colloid Interface Sci. 35 (1971) 346.
[68] K. Gosa, V. Uricanu, E. Pierri, D. Papanagopoulos, A. Dondos, Macromol. Chem. Phys. 201 (2000) 621.
[69] Th. Reinlander, E. Klump, M. Schwuger, J. Disp. Technol. 19 (1998) 379.
[70] S. Rosi, P.F. Luckhman, N. Green, T. Cosgrove, Colloid Surf. A-Physicochem. Eng. Aspects 215 (2003) 11.
[71] N. Salahuddin, A. Rehab, Polym. Int. 52 (2003) 241.
[72] J. Lemmon, J. Wu, M. Lerner, in: J.E. Mark, C.Y.C. Lee, B.A. Bianconi (Eds.), Hybrid Organic–Inorganic Composites, ACS Symposium Series 585, ACS, Washington, DC, 1995, p. 43.
[73] D.J. Chaiko, Chem. Mater. 15 (2003) 1105.
[74] E. Hackett, E. Manias, E.P. Giannelis, Chem. Mater. 12 (2000) 2161.
[75] K.E. Strawhecher, E. Manias, Chem. Mater. 15 (2003) 844.
[76] H.R. Ficher, L.H. Gielgens, T.P.M. Koster, Acta Polym. 50 (1999) 122.
[77] S.S. Hou, T.J. Bonagamba, F.L. Beyer, P.H. Madison, K. Schmidt-Rohr, Macromolecules 36 (2003) 2769.
[78] C.C. Chou, F.S. Shieu, J.J. Liu, Macromolecules 36 (2003) 2187.
[79] Y.H. Shen, Chemosphere 44 (2001) 989.
[80] M.W. Noh, D.C. Lee, Polym. Bull. 42 (1999) 619.
[81] L. Sharma, T. Kimura, Polym. Adv. Technol. 14 (2003) 392.
[82] K.E. Strawhecker, E. Manias, Chem. Mater. 12 (2000) 2943.
[83] K.E. Strawhecker, E. Manias, Macromolecules 34 (2001) 8475.
[84] D.J. Greenland, J. Colloid Sci. 18 (1963) 647.
[85] N. Ogata, S. Kawakage, T. Ogihara, J. Appl. Polym. Sci. 66 (1997) 573.
[86] V. Uricanu, D. Donescu, A.G. Banu, S. Serban, M. Olteanu, M. Dudau, Mater. Chem. Phys. 85 (2004) 120.